IEEE Access
Multidisciplinary : Rapid Review : Open Access Journal

Received 30 October 2023, accepted 20 November 2023, date of publication 23 November 2023, date of current version 15 December 2023.

Digital Object Identifier 10.1109/ACCESS.2023.3336412

RESEARCH ARTICLE

An Adaptive Clustering-Based Distributed Voltage Regulation Scheme for Unbalanced Distribution Systems With Multiple Renewable DGs and OLTCs

RABBAYA AKHTAR[1], REHAN NAWAZ[2], KHAWAJA KHALID MEHMOOD[3,4], SYED BASIT ALI BUKHARI[4], ABDUL WADOOD[5], KASHIF IMRAN[1], TAHIR KHURSHAID[6], AND KI-CHAI KIM[6], (Member, IEEE)

[1]USPCAS-E, National University of Sciences and Technology (NUST), Islamabad 44000, Pakistan
[2]Department of ECE, Air University, Islamabad 44000, Pakistan
[3]Department of Electrical Engineering (EE), Eindhoven University of Technology, 5612 AZ Eindhoven, The Netherlands
[4]Department of EE, The University of Azad Jammu and Kashmir, Muzaffarabad, Azad Jammu and Kashmir 13100, Pakistan
[5]Department of EE, Air University, Kamra Campus, Kamra 45681, Pakistan
[6]Department of Electrical Engineering, Yeungnam University, Gyeongsan 38541, South Korea

Corresponding authors: Rehan Nawaz (rehan._.nawaz@outlook.com), Tahir Khurshaid (tahir@ynu.ac.kr), and Ki-Chai Kim (kckim@ynu.ac.kr)

This work was supported by the Basic Science Research Program through the National Research Foundation of Korea (NRF), funded by the Ministry of Education under Grant NRF-2021R111A3053429.

ABSTRACT In this paper, a real-time adaptive clustering-based distributed voltage regulation scheme is presented for the voltage regulation of unbalanced distribution systems. In the proposed methodology, first, adaptive clusters for the distributed control are formulated based on voltage to injected power sensitivity, and a threshold criterion is designed that limits the size of the clusters to strongly controlled nodes only. Having performed the clustering, a multi-objective optimization problem is solved for power factor optimization within clusters for voltage regulation of all the control zones of the distribution system. Voltage quality factor and voltage unbalance indices are utilized to show the improvements in voltage profile and reduction in voltage unbalance, respectively. Furthermore, for optimally finding the tap positions for multiple OLTCs, another optimization problem is designed. An IEEE 123-node test feeder with multiple wind and solar DGs of varying capacities is used for the simulations, and two test cases with different scenarios are simulated to test the proposed scheme. All the results verify that the proposed scheme effectively regulates the voltage of the unbalanced system without massive remote data requirements and active power curtailment which ensures the stability of the system's voltage profile and prevents OLTC-hunting even in highly dynamic operational scenarios.

INDEX TERMS OLTC tap optimization, power factor optimization, unbalanced distribution systems, voltage regulation.

I. INTRODUCTION

Over the last decade, the numerous benefits associated with the integration of distributed energy resources (DERs) such as reduction in line losses, improvement in voltage profiles and low initial costs have drastically increased the numbers of integrated DERs [1]. Even though the DERs offer a multitude of benefits, they have also posed some significant technical challenges to the host power system such as stability and reliability issues, intermittent generation periods and violations in standard voltage limits [2]. The frequent variations in the voltage profiles demand sophisticated power, control and communication infrastructure [3]. One of the biggest obstacles that further raises the complexity of voltage

The associate editor coordinating the review of this manuscript and approving it for publication was Salvatore Favuzza.

© 2023 The Authors. This work is licensed under a Creative Commons Attribution-NonCommercial-NoDerivatives 4.0 License.
For more information, see https://creativecommons.org/licenses/by-nc-nd/4.0/

regulation schemes of real-world distribution networks is that the real-world power distribution systems are unbalanced systems with each phase having a different magnitude of load and distributed generation on it. This gives rise to varying voltage behaviour between different phases and even different nodes of the same phase; maximum permissible deviation in the voltage from nominal system voltages and the amount of allowed unbalancing within different phases are less than 5% as stated in IEEE Std 1547^{TM} in proper accordance with ANSI C84.1-2006 service voltage limits [4]. Furthermore, in some cases, active power is curtailed for the voltage regulation which results in the financial loss of the DER owners. Therefore, considering the unbalanced real-world distribution systems, in order to utilize already installed voltage control devices such as on-load tap changers (OLTCs) and step voltage regulators (SVR) effectively in the presence of several distributed generators (DGs) to the full extent with minimum amount of remote data, more efficient voltage regulation schemes are required with least dependency on the communication infrastructure.

Extensive research has been conducted to address the problems associated with the voltage regulation of active distribution networks [5], [6]. A fairness-based coordinated power curtailment scheme for mitigation of over-voltage issues is proposed in [7], but it compromises the power generation capability of DGs. In [8], a two-stage centralized voltage regulation scheme is proposed implementing the OLTC and DG VAR control. In [9], a coordinated scheme considering battery storage and OLTC for voltage regulation is proposed. Decoupled voltage and frequency control for a stand-alone microgrid with solar generation DERs is proposed in [10]. Volt/Var control of PVs with scheduling control of OLTCs is proposed in [11]. A novel power electronics device, i.e. soft open point-based decentralized voltage control strategy is proposed using the alternating direction method of multipliers algorithm in [12]. A multi-agent-based decentralized voltage control scheme equipped with consensus protocol is proposed in [13] and [14] that demands interoperability of all system components. A real-time coordination scheme utilizing DGs reactive power control to minimize static voltage regulator operations is presented in [15]. A pinning control scheme of a complex network for voltage stability and generation control is proposed in [16]. A comparative analysis of rule-based and optimization-based coordinated voltage control utilizing linear programming is proposed in [17].

Various sensitivity analysis-based algorithms have also been utilized by different researchers for power network segregation into the smaller control zones [18], [19], [20] e.g. voltage to injected power sensitivity [15], [21], [22], voltage to reactive power sensitivity [23], [24]. A distributed active power control [25] and follow-up scheme along with power quality management for voltage regulation is presented in [26] for balanced systems only. Distribution network sensitivity analysis-based active/reactive power control of inverters for voltage regulation is proposed in [27]. The hierarchical structuring of control zones for the reduced control model is presented for voltage regulation purposes in [28]; however, thresholds for cluster boundaries were not taken into account. A coordinated voltage control scheme to maximize the active power export in highly penetrated active distribution networks is presented in [29]. An adaptive hierarchical clustering-based zone division approach of the power network is presented in [30] and [31]. A forecasting and optimization-based OLTC tap control for multiple OLTCs with high PV penetration in the distribution system to mitigate the voltage rise issue is proposed in [32].

Even though significant progress has been made in the voltage control methods proposed in previous research, some of the research challenges are still substantial. For instance, the aforementioned schemes are designed either for DC grids or for single-phase AC or balanced three-phase systems. As mentioned earlier, the real-world distribution systems are unbalanced in nature; the voltage regulation of real-world unbalanced 3-phase active distribution networks has not been addressed appropriately so far. In addition, some of the schemes deploying centralized control are highly affected by communication lags, and any communication failure may prove devastating for the system. Moreover, some of the schemes utilize active power curtailments for voltage regulation, which may result in financial loss for DG owners. Although in some of the schemes, the distributed control is presented; however, the DGs are not utilized to the maximum extent for the voltage regulation. In some of the cases, zoning is performed by physical division of the network, which overlooks several constraints. Moreover, no criterion has been defined to identify stronger clusters for DG control by limiting the area of control. Furthermore, the coordination between conventional devices i.e. OLTCs and modern controlling agents for effective voltage regulation is yet a grey area.

Considering the aforementioned research gaps, in this paper, a new approach for distributed voltage regulation is proposed for highly unbalanced distribution systems; the proposed scheme is an adaptive clustering-based scheme that not only employs the renewable DGs for voltage regulation but also effectively utilizes OLTCs for the voltage regulation without curtailing active power of the DGs. In the first stage of the scheme, the adaptive clusters/control zones are formed utilizing voltage and reactive power based-sensitivity analysis; a DG control space matrix is formed for each node. Second, the sensitivity parameters are calculated for analysing the Euclidean distance between different nodes. Third, the calculated distances are used for cluster formulation by the agglomerative hierarchical clustering technique. The DGs are considered the central control point of their own cluster. A new boundary threshold criterion is formulated that limits cluster boundaries for a DG to incorporate only strong nodes into clusters.

Following the cluster formation, in the second stage, a multi-objective constrained optimization problem is formulated; for each phase, an objective function minimizes the variations in the voltage of that phase of the unbalanced distribution system. Voltage regulation within the zones is carried out by reactive power optimization to calculate the power factors, leading or lagging, for both solar and wind DGs without curtailing the active power. Voltage quality factor (VQF) and Voltage Unbalance Index(VUI) [33] are evaluated to verify the improvements in the voltage profile and voltage unbalance of the distribution system.

In the final stage of the proposed scheme, another optimization problem is designed which optimally calculates the tap positions of the multiple OLTCs eliminating the hunting effect; the optimization-based tap-selection method is also compared with two conventional tap-selection methods. For testing the efficacy of the proposed methodology, an IEEE 123-node test feeder, which is a large unbalanced test system with multiple OLTCs, is utilized; real wind speed and solar irradiance data are used [34] for modelling multiple wind and solar power DGs of varying capacity installed at different locations and phases of the unbalanced distribution system. In order to validate the proposed scheme, two large test cases with multiple scenarios have also been designed for 24 hours of all four seasons in openDSS.

Some of the key contributions of this research can be summarized as follows:

1) *Unbalanced Distribution Systems:* A new distributed control scheme is proposed that effectively performs voltage regulation of highly unbalanced distribution systems. The voltage unbalance index shows the reduction in the voltage unbalance.
2) *Adaptive Clustering for Voltage Control:* Sensitivity analysis-based clusters are developed for DGs that are updated with time according to the operational scenario of the DG in charge; a new criterion is designed for identifying strong clusters for DG control. The DGs perform voltage regulation within thier clusters without active power curtailment.
3) *Optimization for OLTCs:* Optimal coordination of conventional devices such as OLTCs is also performed with solar and wind DGs for voltage regulation by formulating a separate optimization problem for tap selection that successfully eliminates hunting phenomena.
4) *Intermittent Nature of DERs:* Historical real-wind and solar data have been employed for the modelling of wind and solar DGs. The proposed scheme effectively performed voltage regulation of a large unbalanced test system with multiple DGs of an intermittent nature.

The rest of the paper is organized as follows: Section-II presents the proposed voltage regulation strategy, the clustering technique, reactive power optimization and tap-selection optimization problems. Test systems and test cases are given in Section III, and Section IV provides the results and discussion. Finally, Section-V summarizes the paper.

II. PROPOSED SCHEME

This section presents the details of the proposed scheme; the proposed voltage regulation scheme works for each phase of the distribution network and is mathematically formulated in the following sub-sections.

A. PROBLEM STATEMENT

The voltage profile of a normally operating 3-phase unbalanced distribution system consisting of n nodes can be visualized as (1):

$$\boldsymbol{V} = \left[\boldsymbol{v}_a \ \boldsymbol{v}_b \ \boldsymbol{v}_c\right] \tag{1}$$

where,

$$\boldsymbol{v_j} = \left[v_j{}^1 \ v_j{}^2 \ \ldots \ v_j{}^n\right]^T \ \ \forall j \in [a, b, c]$$

and

$$0.95 \text{ pu} \leq v_j{}^i \leq 1.05 \text{ pu} \ \ \forall v^i \in \boldsymbol{v_j}, \ i \in \{1, 2, 3, \ldots, n\} \tag{2}$$

$\boldsymbol{V}$ is the matrix representation of the voltage profile of n-node 3-phase unbalanced distribution feeder; each column of the matrix represents the voltages of a single phase. If a node is missing from a phase, a zero will be placed for that column entry in $\boldsymbol{V}$. Therefore, the dimensions of $\boldsymbol{V}$ are $n \times 3$. Any i-th row of the matrix $\boldsymbol{V}$ shows the voltage profile of i^{th} node with per unit node voltages of each phase $v_a{}^i$, $v_b{}^i$, and $v_c{}^i$.

The effect on voltages of different nodes of distribution feeder due to the integration of DGs depends on various factors such as the point of DG-coupling, linkage of other nodes to that point and varying power flow conditions in real power systems. Therefore, having integrated the DGs into a 3-phase unbalanced distribution system, the new varied voltages can be expressed as:

$$\boldsymbol{V}_{new} = \left[\boldsymbol{v}_a + \boldsymbol{\delta}_a \ \boldsymbol{v}_b + \boldsymbol{\delta}_b \ \boldsymbol{v}_c + \boldsymbol{\delta}_c\right] \tag{3}$$

where, $\boldsymbol{\delta_j}$ is an $n \times 1$ vector representing the variations of voltages in phase 'j' due to power injections of DGs interfaced with the feeder. These deviations due to DG injections are sometimes large enough that some of the node voltages exceed the safe operating voltage limits as described in (2).

B. STAGE 1: ADAPTIVE HIERARCHICAL CLUSTERING

The proposed adaptive clustering approach constructs the clusters/zones for reactive power optimization; the number of control zones is equal to the active DGs at that time instant integrated with the system. Furthermore, the span of a control zone is proportional to the impact of DG-injections on nodal voltages and controllability of DG-selected as its zone controller considering its operational constraints.

The time step simulations for 24 hours are run to depict the dynamic nature of the problem. Each node n^i consists of different numbers of phases as shown in (4):

$$n^i \subset n_j \qquad j \in [a, b, c] \tag{4}$$

Assuming a phase j with **n** nodes, out of which d nodes are hosting DGs on them, where d can be variable for each phase as shown in (5):

$$\boldsymbol{g_j} = \left[dg_1 \; dg_2 \; \ldots \; dg_d\right] \tag{5}$$

Here, g_j is a row vector that shows the number of DGs installed at phase j of the unbalanced distribution system.

The ability of a DG at i^{th} node to control the voltage profile of n_j nodes, excluding externally controlled nodes with zero VQ sensitivity, is evaluated by its impact shown in (6):

$$\boldsymbol{s}_i = \left(\frac{\partial v_1}{\partial Q_i} \; \frac{\partial v_2}{\partial Q_i} \; \cdots \; \frac{\partial v_{n_j}}{\partial Q_i}\right) \qquad i \in \boldsymbol{g_j} \tag{6}$$

These sensitivity vectors are obtained by simulating a unit DG at each member node of vector $\boldsymbol{g_j}$ resulting in a $n_j \times d$ dimensional DG-control space matrix as shown in (7):

$$\boldsymbol{S_{DG}} = \begin{bmatrix} \frac{\partial v_1}{\partial Q_1} & \frac{\partial v_1}{\partial Q_2} & \cdots & \frac{\partial v_1}{\partial Q_d} \\ \frac{\partial v_2}{\partial Q_1} & \frac{\partial v_2}{\partial Q_2} & \cdots & \frac{\partial v_2}{\partial Q_d} \\ \vdots & \vdots & \ddots & \vdots \\ \frac{\partial v_{n_j}}{\partial Q_1} & \frac{\partial v_{n_j}}{\partial Q_2} & \cdots & \frac{\partial v_{n_j}}{\partial Q_d} \end{bmatrix}_{n_j \times d} \tag{7}$$

Because different nodes have different sensitivity of coupled DGs injection, the numerical values in (7) have large variations in the sensitivity values which is represented in the heights of the dendrograms in the hierarchical clustering; closely linked nodes will have smaller heights and would not be visible in the dendrogram. In order to normalize the variations in the values, the control space is then transformed to sensitivity parameters by implementing an element-wise operation as given in (8). As the sensitivity values are between 0 and 1, the negative log is taken to obtain positive values from (8):

$$\boldsymbol{S^o_{DG}} = -\log_{10}(\boldsymbol{S_{DG}}) \tag{8}$$

Now to develop clusters, pairwise Euclidean distance is calculated between nodes based on sensitivity parameters of $\boldsymbol{S^o_{DG}}$. Pairwise Euclidean distance calculation between node x and y is shown in (9):

$$Dist_{xy} = \sqrt{\sum_{i=1}^{d} \left(\boldsymbol{S^o_{DG(x,i)}} - \boldsymbol{S^o_{DG(y,i)}}\right)^2} \tag{9}$$

The obtained distances are employed as a base to evaluate ward criterion linkages, which is an error sum of squares (ESS) linkage function-based technique used for agglomerative hierarchical clustering. Thereafter, agglomerative hierarchical clustering of closely linked nodes is performed considering the distance between clusters evaluated by the ESS linkage function given in (10):

$$ESS(x) = \sum_{i=1}^{Nx} \left| x_i - \frac{1}{Nx} \sum_{j=1}^{Nx} x_j \right|^2 \tag{10}$$

The distance between two clusters x and y can be evaluated by (11):

$$D(x, y) = ESS(z) - [ESS(x) + ESS(y)] \tag{11}$$

where, z represents the resulting combined cluster of x and y.

Finally, the dendrograms are drawn to visualize the resulting clusters.

1) CLUSTERING BOUNDARY THRESHOLD CRITERION

In this scheme, clusters are formed with the DG as the central point/brain of its cluster based on the smallest linkages formed between the nodes; the cluster's boundary for a DG is decided on how abruptly the linkage span changes on each step of cluster formation. At this point, it is important to mention that the proposed clustering scheme is adaptive in that whenever the operational scenario changes in the unbalanced distribution system, new clusters are formed based on the available power of the DGs for each phase.

On a phase 'j' with d number of DGs, there are $\boldsymbol{\psi}$ node linkage paths formed for d number of DGs as shown in (12):

$$\boldsymbol{\psi} = [\boldsymbol{\psi_1}, \boldsymbol{\psi_2}, \boldsymbol{\psi_3}, \; \ldots \boldsymbol{\psi_d}] \tag{12}$$

ψ_x contains the complete linkage path from single host node $x \in g$ to the top of hierarchical tree. Considering x-th and y-th DGs, the bottom-up stepwise linkage path including nodes for both is represented in (13) and (14), respectively.

$$\boldsymbol{\psi_x} = [n_1, n_2, n_3, \; \ldots n_{l_N}] \tag{13}$$

$$\boldsymbol{\psi_y} = [m_1, m_2, m_3, \; \ldots m_{l_M}] \tag{14}$$

where, l_N and l_M represent the total number of node-linkages included in the path originating from x-th and y-th DG's hosting nodes leading to the top of the hierarchical tree. To identify strongly controlled nodes for the DGs, the index of the intersection of $\boldsymbol{\psi_x}$ and $\boldsymbol{\psi_y}$ are picked up in the form of array $\boldsymbol{\tau_{xy}}$ as shown in (15):

$$\boldsymbol{\tau_{xy}} = idx(\psi_x \cap \psi_y) \tag{15}$$

The nodes common to both DGs would be the weak nodes and will be influenced by both DGs and hence not included in any particular cluster. The rest of the nodes i.e., stronger nodes will be assigned to a particular DG's cluster with comparatively stronger linkage. A $\boldsymbol{\xi}$ matrix of $d \times d$ dimension is formed by picking the corresponding array entries from ψ_x and ψ_y for identifying nodes following (16) emphasizing that ξ_{xy} is symmetrical where diagonal/self linkages between nodes are infinite, whereas mutual linkages/off-diagonals show connectivity between corresponding node pairs.

$$\xi_{xy} = \begin{cases} \psi_x(\min(\boldsymbol{\tau_{xy}}) - 1) & x \neq y \\ \text{inf} & \text{Otherwise} \end{cases} \tag{16}$$

Minimum value of each row vector of $\boldsymbol{\xi}$ i.e. $\boldsymbol{\xi_x}$ represents the thresholds for x-th DG zone in hierarchical tree as presented in (17):

$$th_x = \min(\boldsymbol{\xi_x}) \tag{17}$$

Hence, the proposed threshold criterion ensures that each DG's cluster has strong intra-zonal node linkages with weak inter-zonal dependency; the zones are dynamically updated according to the time scenario of DGs and are adaptive enough to address the issues caused by the intermittent nature of DGs and variable power injections pertaining to ambient conditions.

C. STAGE 2: REACTIVE POWER OPTIMIZATION BY POWER FACTOR CONTROL

In Stage 2, after cluster formation, the DGs smartly utilize their reactive power injection and absorption capability by power factor manipulation for voltage regulation of its own cluster and ultimately the whole unbalanced distribution system. The optimal power factor allocation to the zonal controllers is based on constrained multi-objective optimization. If $\boldsymbol{\phi}_t^j$ is an array of power factors, leading or lagging, at any time instant 't' for all the DGs for phase 'j' of the unbalanced distribution system, the decision variables can be represented by (18):

$$\boldsymbol{\phi}_t^j = \left[\phi^j_{(1,t)}\ \phi^j_{(2,t)}\ \phi^j_{(3,t)}\ \ldots\ \phi^j_{(z_c,t)} \right] \quad t \in T \tag{18}$$

where, z_c is the number of potentially active DGs at a time 't' designated as zonal controllers. If there are 'c' number of zones constructed for a phase 'j' at time instant t, consisting of different number of nodes depending upon the ability of a DG as a zone controller, the control zones can be expressed as (19):

$$\boldsymbol{z}_t^j = \left[z^j_{(1,t)}\ z^j_{(2,t)}\ z^j_{(3,t)}\ \ldots\ z^j_{(c,t)} \right] \quad t \in T \tag{19}$$

The multi-objective optimization tends to minimize the voltage fluctuation of member nodes of each cluster from standard reference voltage v_{ref} for all the phases of the unbalanced network by optimally selecting the power factor for each DG based on its own zone's voltage profile as depicted in (20) and (21):

$$\min(f_1(\phi^j_{(1,t)}), f_2(\phi^j_{(2,t)}), \ldots f_{z_c}(\phi^j_{(z_c,t)})) \quad j \in [a,b,c] \tag{20}$$

$$f_i(\phi^j_{(i,t)}) = \sum_{i=1}^{n_i} \left\| V_{ref} - v^j_{(c,i,t)} \right\| \quad i = 1, 2, \ldots z_c \tag{21}$$

$$\text{subject to } V_i^{j(\min)} < v^j_{(c,i,t)} < V_i^{j(\max)} \quad \forall_i,\ t \in T, \ j \in [a,b,c] \tag{22}$$

$$\phi^{\min} < \phi^{j(SG)}_{(i,t)} < \phi^{\max} \quad \phi^{j(SG)}_{(i,t)} \subseteq \phi_t^j, \ \forall_c,\ t \in T \tag{23}$$

$$\phi^{\min} < \phi^{j(WG)}_{(i,t)} < \phi^{\max} \quad \phi^{j(WG)}_{(i,t)} \subseteq \phi_t^j, \ \forall_c,\ t \in T \tag{24}$$

$$v^j_{(c,i,t)} = 0 \quad \forall i \notin c,\ \forall c,\ t \in T \tag{25}$$

$$init(\boldsymbol{\phi}_t^j) = \boldsymbol{\phi}_{t-1}^j \quad t \in T \tag{26}$$

$$P^j_{(c,t)}(WG) > 0 \quad \forall_c,\ t \in T \tag{27}$$

$$P^j_{(c,t)}(SG) > 0 \quad \forall_c,\ t \in T \tag{28}$$

where, $v^j_{(c,i,t)}$ is the voltage of i^{th} node in c^{th} zone for time instant 't' and phase 'j', consisting of total n_j nodes. $\phi^{(i,t)}_{j(SG)}$ is the power factor of i^{th} solar DG at time instant 't' for phase 'j'; $\phi^{(i,t)}_{j(WG)}$ is the power factor of i^{th} wind DG at time instant 't' for phase 'j', and T is the total time. Constraints in (22)–(24) specify boundary limits for the voltage and power factors of solar and wind DGs. Constraint (25) emphasizes that only voltages of only member nodes of clusters are utilized for the optimization of that specific cluster. Constraint (26) states that the operational states of the previous time step are the initial solutions for the next time step. Finally, constraints in (27) and (28) restrict that only active DGs can participate in the optimization.

1) VOLTAGE QUALITY FACTOR (VQF)

The accuracy achieved by regulatory action is measured in terms of the minimization of percentage deviations of the nodal voltage from the reference voltage that represents a complete profile of a phase as indicated by voltage quality factor in (29):

$$\eta_t^j = \left(1 - \frac{1}{n_j} \sum_{i=1}^{n_j} \left\| V_{ref} - v^j_{(i,t)} \right\| \right) \times 100 \quad j \in [a,b,c] \tag{29}$$

where 'j' can be any of the three phases and η_j^t is the overall voltage quality of that phase for time instant 't'. The higher the value of the voltage quality factor, the more is the accuracy of the proposed voltage regulation scheme.

2) VOLTAGE UNBALANCE INDEX (VUI)

As the proposed scheme is designed for the unbalanced distribution systems, a VUI is employed to measure the magnitude of unbalancing in the voltage of i-th 3-phase-node at time 't' as given in (30):

$$VUI_{(i,3,t)} = \left(\frac{Max.\ deviation\ from\ average}{Average\ value} \right) \times 100 \tag{30}$$

D. STAGE 3: OLTC TAP SELECTION

Since OLTCs were used as primary voltage regulation devices in the conventional distribution systems, in Stage 3, a new optimal coordination strategy is proposed for integrating OLTCs with the proposed adaptive clustering-based distributed voltage control scheme. To select the best method for tap selection and communication of OLTCs, a comparative analysis of three different decision criteria for tap selection is performed.

1) AUTONOMOUS TAP SELECTION (OLTC-T2) CRITERION

The autonomous control is based entirely on voltage monitoring of the secondary node of the OLTC only. If there are 'r' number of OLTCs in the system with their compensators on different phases of the system, considering ns_l number of nodes on secondary side of the l^{th} OLTC with s_l° being the host node of OLTC secondary, the tap selection criterion is shown in (31):

$$\lambda = (v_{sl}^{\circ} - V_{ref}) \tag{31}$$

$$n_{Tap}^{(h)} = \begin{cases} n_{Tap}^{(h-1)} - \kappa & \text{for } \lambda \geq \Delta V_{Tap} \\ n_{Tap}^{(h-1)} + \kappa & \text{for } \lambda \leq -\Delta V_{Tap} \\ n_{Tap}^{(h-1)} & \text{otherwise} \end{cases} \tag{32}$$

where, ΔV_{Tap} is the amount of change of voltage associated with one tap shift, and n_{Tap}^{h} is the current tap position w.r.t n_{Tap}^{h-1} i.e. previous tap position. κ is the number of tap shifts required based on the amount of voltage deviation as shown in (33):

$$\kappa = \frac{\lambda}{\Delta V_{Tap}} \tag{33}$$

2) REMOTE TAP SELECTION (OLTC-T1) CRITERION

This method is conventionally used for OLTC-tap selection; in this approach, the same control, described in the preceding sub-section, is implemented with farthest node $s_l^{ns_l}$ voltages. However, both controls have the limitation that a single bus in the active distribution network may not accurately represent the voltage profile of the whole unbalanced distribution system. Therefore, it is most suitable to adapt an optimal coordinated OLTC tap selection scheme.

3) PROPOSED COORDINATED TAP SELECTION SCHEME (OLTC-T3)

The coordinated scheme optimally selects tap positions based on a wider scenario of secondary side nodes of respective phase to minimize net voltage deviations at the secondary side of each OLTC installed on different phases of the unbalanced distribution system.

The secondary side node voltages of l^{th} OLTC at time instant 't' can be represented by $\boldsymbol{vs}_{(l,t)}$ as:

$$\boldsymbol{vs}_{(l,t)} = [vs_{(l,t)}^{\circ}, vs_{(l,t)}^{1}, vs_{(l,t)}^{2} \ldots vs_{(l,t)}^{ns_l}] \tag{34}$$

A constrained optimization problem is formulated to minimize the voltage variations on the secondary side of all the OLTCs installed in the system to select the taps as provided in (35) and (36):

$$\min(f_1(n_{(Tap,t)}^{1}), f_2(n_{(Tap,t)}^{2}), \ldots f_r(n_{(Tap,t)}^{r})) \tag{35}$$

$$f_l(n_{(Tap,t)}^{l}) = \sum_{i=1}^{ns_l} \left(\sqrt{(vs_{(l,t)}^{i} - V_{ref})^2} \right)$$

$$\text{for } l = 1, 2, \ldots r \tag{36}$$

$$\text{subject to } n_{(Tap,t)}^{\min} \leq n_{(Tap,t)}^{l} \leq n_{(Tap,t)}^{\max} \quad \forall_l,\ t \in T \tag{37}$$

$$vs_{(l,t)}^{i} = 0 \quad \forall i \notin l,\ t \in T \tag{38}$$

$$init(\boldsymbol{n}_{(Tap,t)}) = \boldsymbol{n}_{(Tap,t-1)} \quad t \in T \tag{39}$$

$$n_{(Tap,t)}^{l} \in \mathbb{Z} \tag{40}$$

where,

$$\boldsymbol{n}_{(Tap,t)} = [n_{(Tap,t)}^{\circ}, n_{(Tap,t)}^{1}, n_{(Tap,t)}^{2}, \ldots, n_{(Tap,t)}^{c}]$$

Constraint in (37) shows that the possible tap positions are physically constrained by maximum n_{Tap}^{max} and minimum n_{Tap}^{min} numbers of taps. Constraint (38) shows that only secondary side node voltages affect the tap position. Constraint (39) states that the previous tap position is a base point for the next decision. Finally, to generate feasible solutions for tap-positons, (40) ensures that only integers are generated within the limits defined by (37). Although the communication dependency is a bit higher in this approach, however, it is the most suitable control as the OLTC tap shift has widespread effects along the feeder. Also, the power factor regulation prior to tap selection of OLTCs provides significant relief from the hunting effect, resulting from the high disparity operation of DGs and loads at the cost of compromising the time taken for tap selection.

Hence, the proposed decentralized voltage regulation scheme's primary focus is to encapsulate the distribution feeder's voltage profile within safe operational limits as per IEEE standards, even under the influence of multiple intermittent DERs and load variation, with minimum dependency on the communication infrastructure and remote measurements. The conventional control equipment, i.e., OLTCs are incorporated with remedial measures to avoid hunting and independent phase voltage regulation. At this stage, it is worth mentioning that the proposed algorithm assumes an n phase DG is equivalent to n single-phase DG units having separate phase interface control with its capacity equally divided into n units. Time delay for OLTC tap shift is utilized for power factor optimization of DGs so that there may not be any unnecessary tap shifts.

III. TEST SYSTEM AND TEST CASES

In order to verify the efficacy of the proposed distributed voltage regulation scheme, a standard IEEE 123-node test feeder has been used for developing test cases using openDSS interfaced with MATLAB for time-based simulations; the test feeder has a considerable amount of renewable solar and wind power generation units of sizable capacity. The probabilistic normalized dispatch curves for PV and wind DGs along with the load demand variation curve, based on real on-site data of Texas and New Mexico taken from the NREL database, are used [34]. Both of the designed optimization problems are solved using MATLAB's Global Optimization Toolbox. The DGs are hosted at random nodes of the feeder, and two different test case scenarios are explored through time-based simulations to verify the validity of the proposed control scheme for varying operational scenarios. Case I considers unbalanced loads with similar DGs integrated at all three phases, whereas Case II explores unbalanced loads with DG integrations varying in number and host node location on each phase.

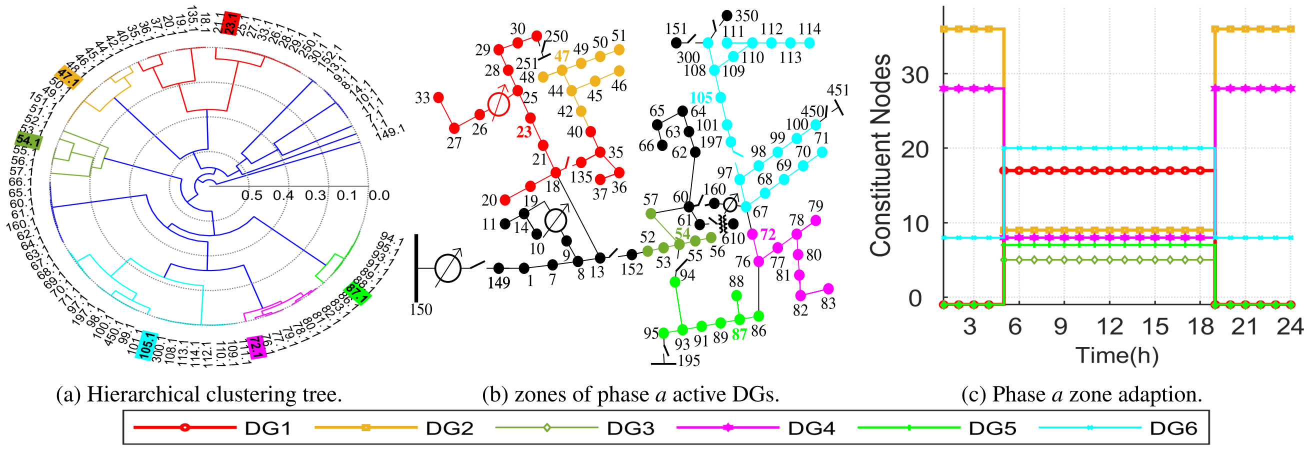

(a) Hierarchical clustering tree. (b) zones of phase *a* active DGs. (c) Phase *a* zone adaption.

FIGURE 1. Phase-a distributed control scenario. (a) Hierarchical tree dendrogram showing colour-coded clusters of potentially active DGs with highlighted host node. (b) Zonal visualization of IEEE 123-node test feeder. (c) Adaptation of zone span according to operational scenario.

IV. RESULTS AND DISCUSSION

This section provides the results and discussion of the test cases presented in the preceding section.

TABLE 1. Specifications and placement details of DGs for Case-I. (Node name.a.b.c specifies the containing phases).

DG	Host Node	KW rating/phase	Class
DG-1	23.a.b.c	300	Solar
DG-2	47.a.b.c	500	Wind
DG-3	54.a.b.c	400	Solar
DG-4	72.a.b.c	600	Wind
DG-5	87.a.b.c	300	Solar
DG-6	105.a.b.c	500	Wind

A. TEST CASE-I

In the first test scenario, six DGs per phase are interfaced on similar nodes of each phase to imitate the effect of multi-phase DGs with separate interface controls for each phase. The specifications of DGs are given in Table 1. The simulation results of a typical spring day at 1 PM are presented in Figure 1a to analyze the performance of proposed adaptive clustering algorithm for an unbalanced distribution network. As described in Section-II-A, all the following results and discussion deal with all 3-phases separately. Figure 1a shows the resulting hierarchical tree clusters for phase-*a* along with highlighted colour-coded zones for each DG with DG appointed as its zone controller at 1 PM. The clusters formed in Phase a of the distribution system at 1 PM can be visualized in the IEEE 123-node feeder in Figure 1b. In case of any violations in the voltage limits, the clusters update themselves in that the total number of nodes in a cluster is different depending upon the ability of the DG to control the voltage of the zone; the dynamic nature of adaptive clustering for average spring season day scenario is prominent in zone span representation in Figure 1c. It is evident from the figure that the number of nodes in clusters is changing based on the ability of DGs to control the voltage of the distribution system at that time period; however, the number of clusters formed depends on the number of active DGs installed in the system. Same results obtained for Phases b and c are shown in Figure 2 and Figure 3 respectively.

Figure 4 shows normally operational conventional feeder voltage profiles for each phase without DG displaying unidirectional power flow. Once the DGs actively inject powers into the system, the over-voltage issue at effected nodes arises as evident from the VQF dropping to 95.97%, 94.78%, 95.93% for respective phases. In Figure 6, OPF represents voltage after optimal power factor allocation; OLTC-T3 is coordinated control. OLTC-T2 is autonomous, and OLTC-T1 is based on remote measurement of the far end. After optimal power factor allocation to DGs through the proposed algorithm, the nodal voltages achieve VQFs of 99.81%, 99.86% and 99.76% for phases a, b, and c, respectively. The optimization resumes for the next time state with the operational statistics of the previous time state as its initial solutions. Once the power factors are optimized, and the time delay for OLTCs is over, the tap selection of OLTCs is completed according to different decision variables opted in OLTC-T1, OLTC-T2, and OLTC-T3 criteria as explained in Section-II-D. The resulting improvements in the feeder voltages can be seen in Figure 6 with resulting VQFs of 99.76%, 99.87% and 99.84% for phases a, b, and c, respectively. There are four multi-phase OLTCs with compensators on different phases. Here, each compensator is treated as an individual control agent for its own phase, and a total of seven OLTCs are considered for tap selection based on three techniques as explained in Section II-D. The comparison of a number of tap shift operations resulting from above mentioned criteria during time simulation is shown in Figure 5. The other two techniques for tap selection of OLTCs are also simulated, and the resulting tap positions are displayed in the same figure for comparison. The coordination-based optimization technique for tap selection (OLTC-T3) achieves

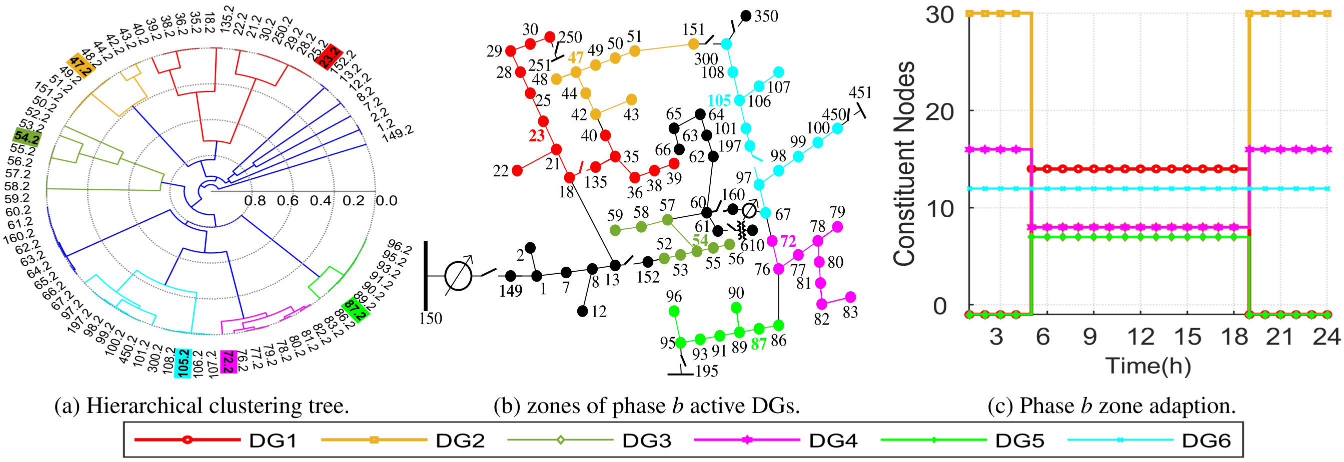

(a) Hierarchical clustering tree. (b) zones of phase *b* active DGs. (c) Phase *b* zone adaption.

FIGURE 2. Phase-b distributed control scenario. (a) Hierarchical tree dendrogram showing colour-coded clusters of potentially active DGs with highlighted host node. (b) Zonal visualization of IEEE 123-node test feeder. (c) Adaptation of zone span according to operational scenario.

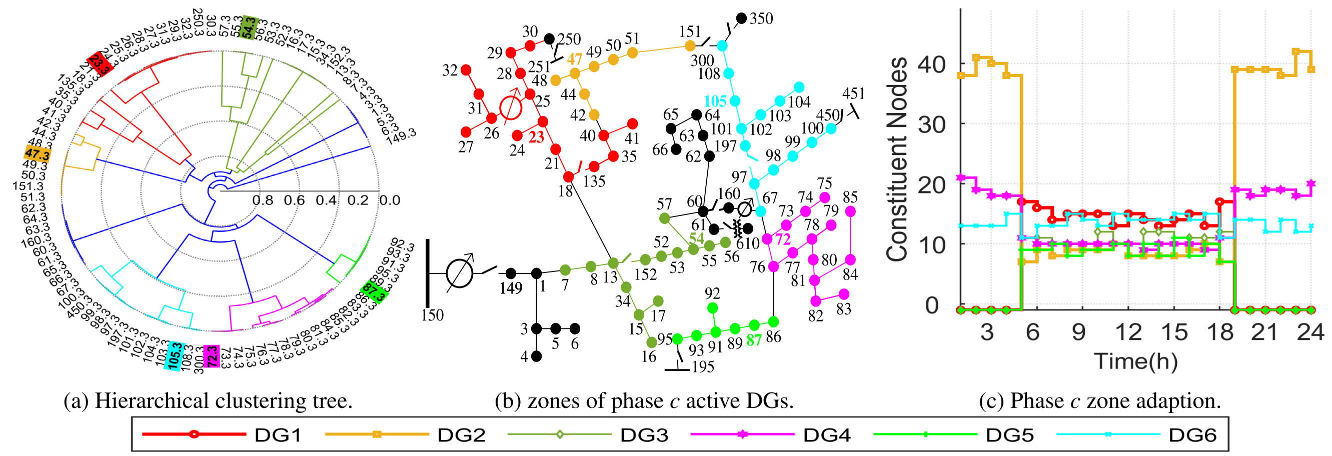

(a) Hierarchical clustering tree. (b) zones of phase *c* active DGs. (c) Phase *c* zone adaption.

FIGURE 3. Phase-c distributed control scenario. (a) Hierarchical tree dendrogram showing colour-coded clusters of potentially active DGs with highlighted host node. (b) Zonal visualization of IEEE 123-node test feeder. (c) Adaptation of zone span according to operational scenario.

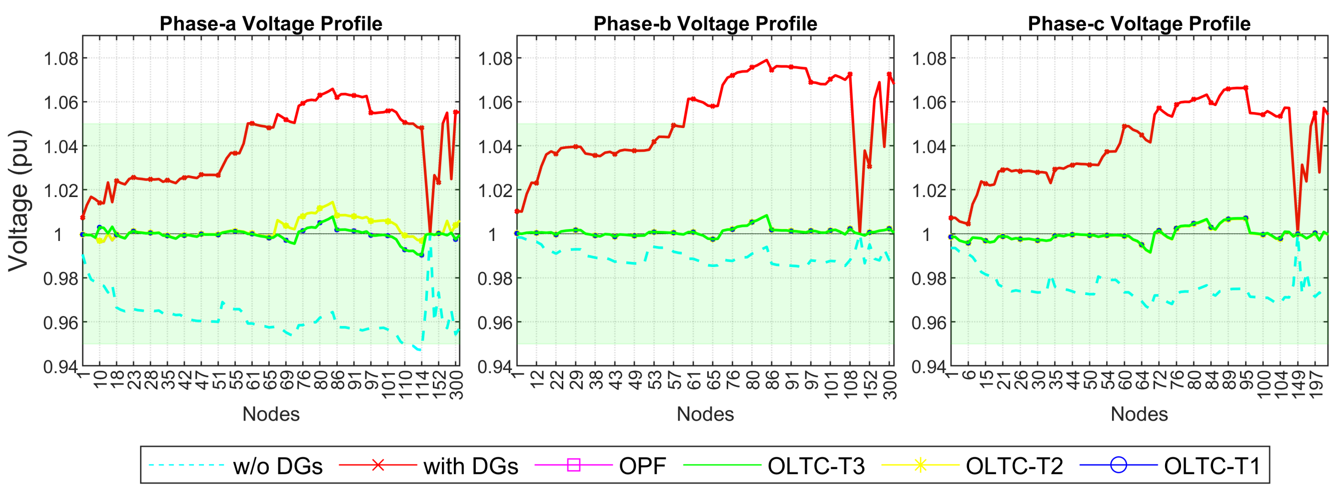

FIGURE 4. Phase-wise voltage profiles before and after different regulation stages.

the highest VQF with minimum tap shifts, while the other two schemes, T2 and T1, achieve lower VQF values. Therefore, in overall performance, OLTC-T3 is considered the best way to select taps for OLTCs optimally.

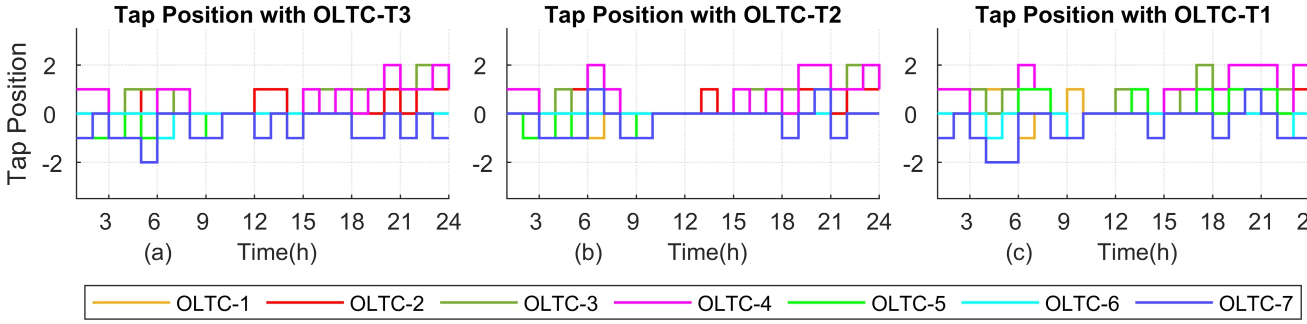

FIGURE 5. (a). OLTCs' tap positions by OLTC-T3 (b). OLTCs' tap positions by OLTC-T2. (c). OLTCs' tap positions by OLTC-T1.

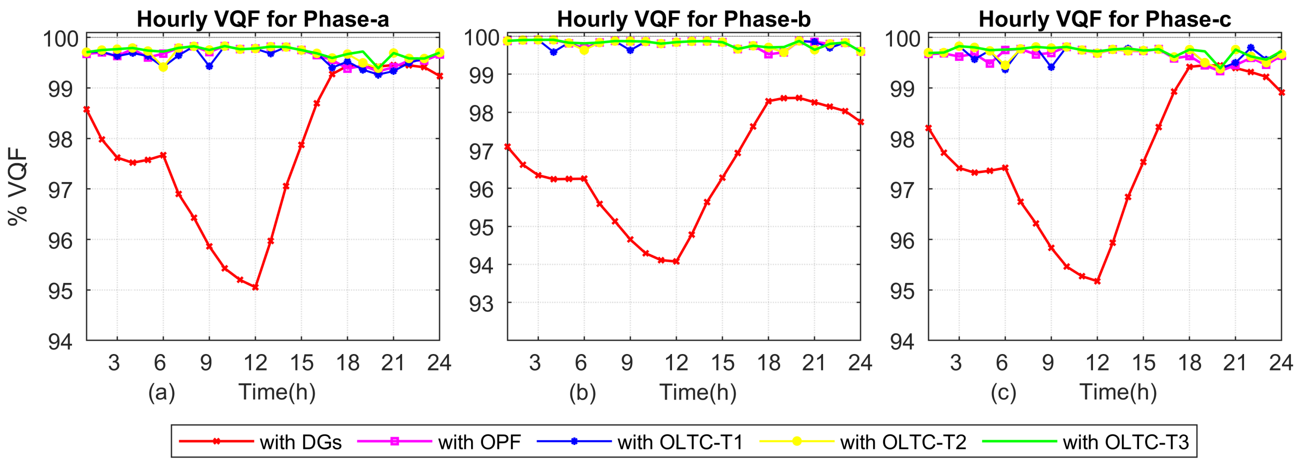

FIGURE 6. Stage wise Voltage Quality Factor (VQF) analysis. (a). phase *a* (b). phase *b* (c). phase *c*.

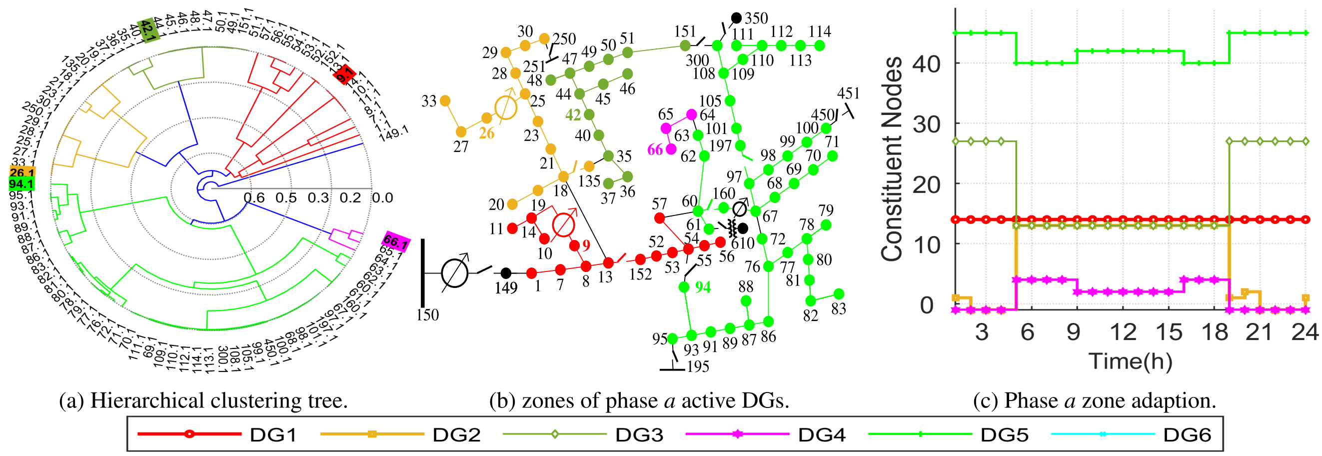

FIGURE 7. Phase-a distributed control scenario. (a) Hierarchical tree dendrogram showing colour-coded clusters of potentially active DGs with highlighted host node. (b) Zonal visualization of IEEE 123-node test feeder. (c) Adaptation of zone span according to operational scenario.

B. TEST CASE-II

For the second test case, multiple single-phase DGs are integrated into each phase of the test system varying in numbers, classes and generation capacities. The specifications of DGs are listed in Table 2. The placement of DGs in close neighbourhoods along with unbalanced injections test the robustness of the proposed control strategy.

For performance comparison and evaluation on both test cases of the scheme, the same time period, 1 PM, is considered for the simulations. The resulting clusters for voltage control for Phase-a obtained from the proposed scheme at 1 PM are shown in Figure 7a. The same clusters can be visualized in the IEEE 123 feeder in Figure 7b. Similar to Case-I, Figure 7c shows how the zones adapt themselves

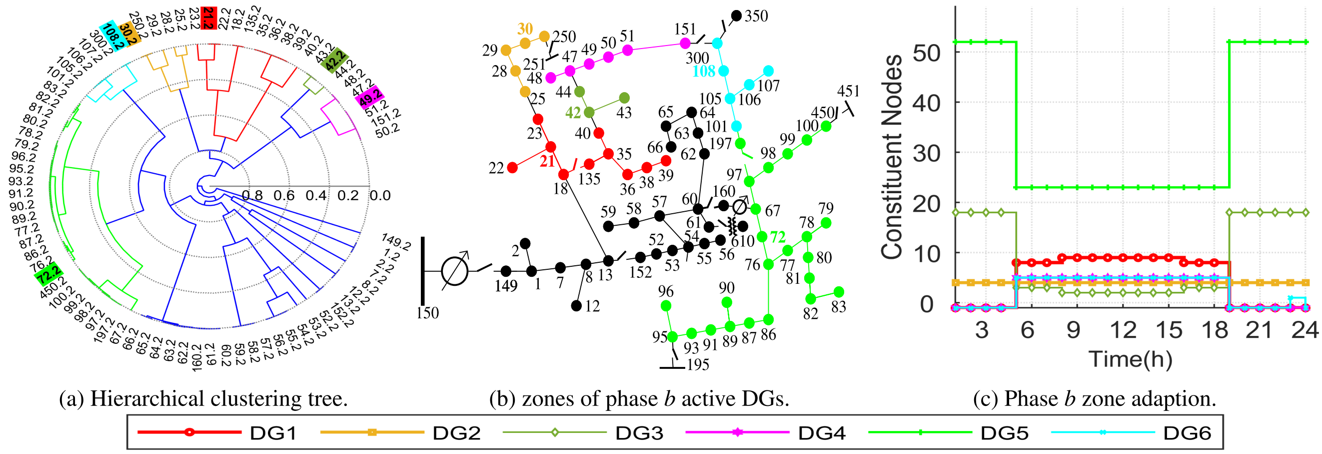

(a) Hierarchical clustering tree. (b) zones of phase *b* active DGs. (c) Phase *b* zone adaption.

FIGURE 8. **Phase-b distributed control scenario. (a) Hierarchical tree dendrogram showing colour-coded clusters of potentially active DGs with highlighted host node. (b) Zonal visualisation of IEEE 123-node test feeder. (c) Adaptation of zone span according to operational scenario.**

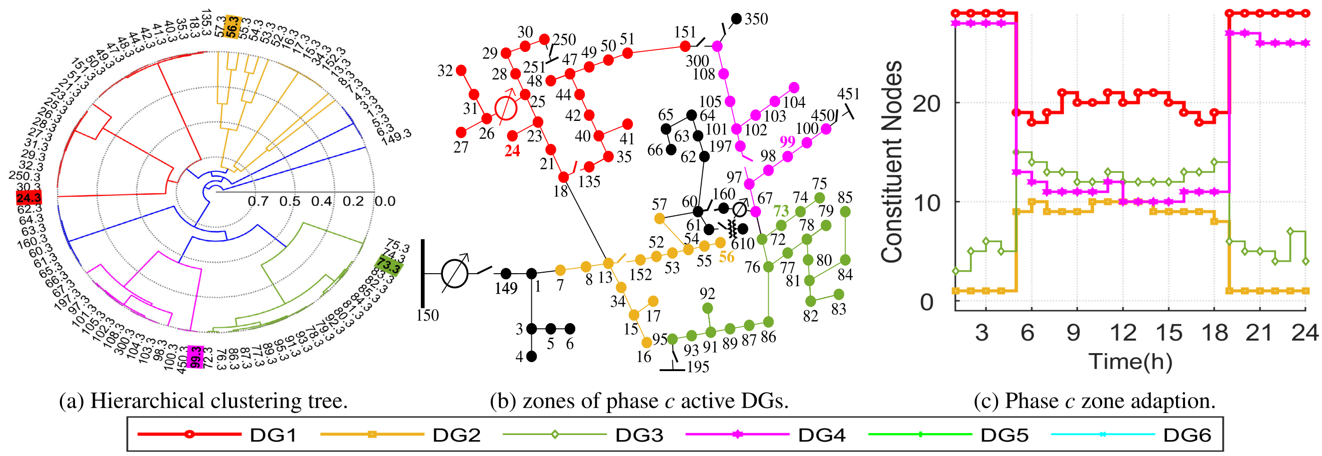

(a) Hierarchical clustering tree. (b) zones of phase *c* active DGs. (c) Phase *c* zone adaption.

FIGURE 9. **Phase-c distributed control scenario. (a) Hierarchical tree dendrogram showing colour-coded clusters of potentially active DGs with highlighted host node. (b) Zonal visualisation of IEEE 123-node test feeder. (c) Adaptation of zone span according to operational scenario.**

TABLE 2. **Specifications and placement details of DGs for Case-II. (Node name.a.b.c specifies the containing phases).**

DG	Host Node	Phase	KW rating	Class
DG-1	9	a	300	Wind
DG-2	26	a	500	Solar
DG-3	42	a	500	Wind
DG-4	66	a	400	Solar
DG-5	94	a	600	Wind
DG-6	21	b	500	Solar
DG-7	30	b	500	Wind
DG-8	42	b	400	Wind
DG-9	49	b	600	Solar
DG-10	72	b	300	Wind
DG-11	108	b	600	Solar
DG-12	24	c	500	Wind
DG-13	56	c	500	Solar
DG-14	73	c	400	Solar
DG-15	99	c	600	Wind

dynamically to the changes in DG operational behavioural changes throughout the day. The number of the DGs installed in Phase-a as listed in Table 2 is five; as a result, the number of clusters formed is also five for Phase a. Once a DG becomes ineffective due to intermittency factors, other neighbouring DGs with a strong reaching impact on the dissolved cluster take over constituent nodes considering their influencing power. As mentioned earlier, the same results are obtained for Phases b and c as shown in Figure 8 and Figure 9 respectively.

The voltage profile of the feeder is displayed in Figure 10 for normal operation without any DGs. In addition, the voltage disturbances with DG integration are highlighted with respective VQFs of 96.96%, 93.45%, and 97.89% for Phases a, b and c, respectively. In Figure 12, OPF represents voltage after optimal power factor allocation, OLTC-T3 is optimization-based; OLTC-T2 is autonomous, and OLTC-T1 is based on remote measurement of the far end. The regulated voltage profile after optimal power factor allocation to DGs according to the proposed scheme is shown with improved VQFs of 99.57%, 99.42%, and 98.42% achieved for each phase, respectively. Finally, the OLTC tap selection is made through each of the three proposed schemes, and the results are displayed in the same figure for comparison.

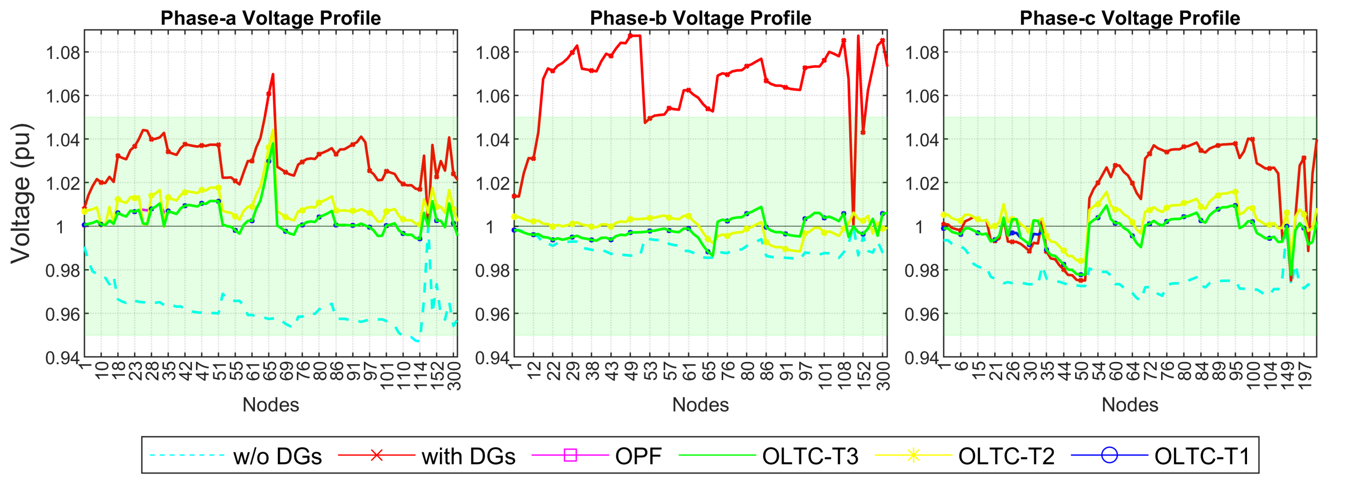

FIGURE 10. Phase-wise voltage profiles before and after different regulation stages.

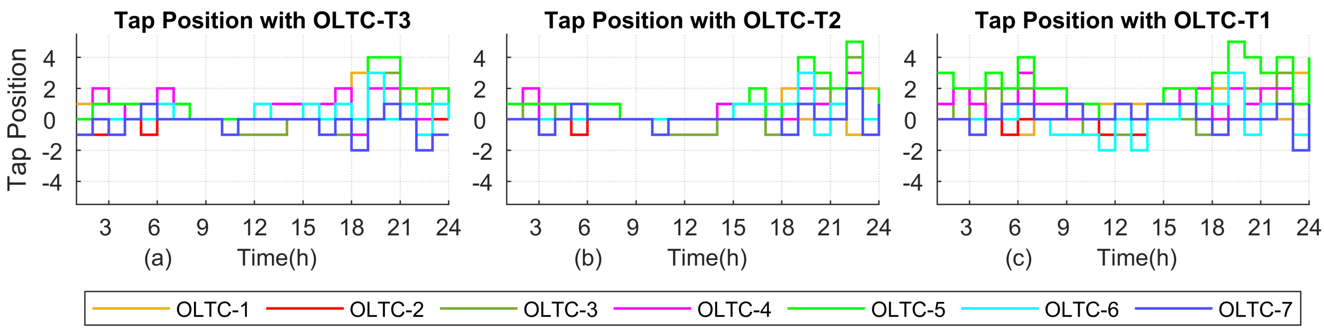

FIGURE 11. (a). OLTCs' tap positions by OLTC-T3 (b). OLTCs' tap positions by OLTC-T2. (c). OLTCs' tap positions by OLTC-T1.

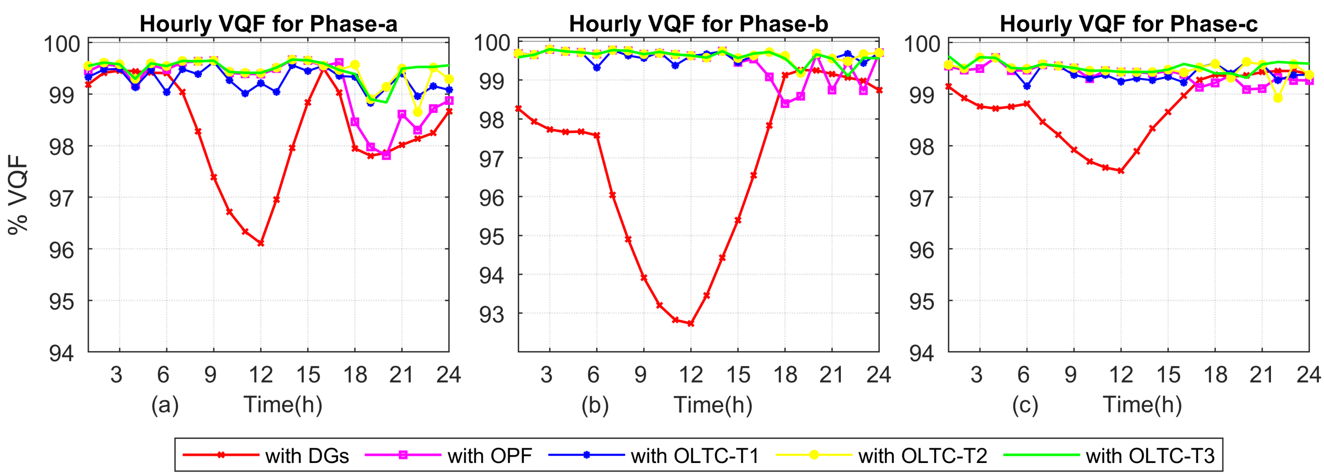

FIGURE 12. Stage wise Voltage Quality Factor (VQF) analysis. (a). phase *a* (b). phase *b* (c). phase *c*.

The resulting VQF of OLTC-T1, OLTC-T2, and OLTC-T3 are 99.04%, 99.51%, 99.51% for phase-a, 99.67%, 99.57%, 99.57% for phase-b and 99.31%, 99.42%, 99.42% for phase-c, respectively. The selected tap positions for OLTCs resulting from all three techniques are presented in Figure 11. For stepwise analysis of improvements in voltage quality, the VQFs for each phase before and following each regulatory action are displayed in Figure 12.

Finally, the variations in voltage unbalance of 3-phase buses in both cases are displayed in Figure 13; the results of VUI values after applying the proposed schemes are compared with no control scheme values. It can be seen

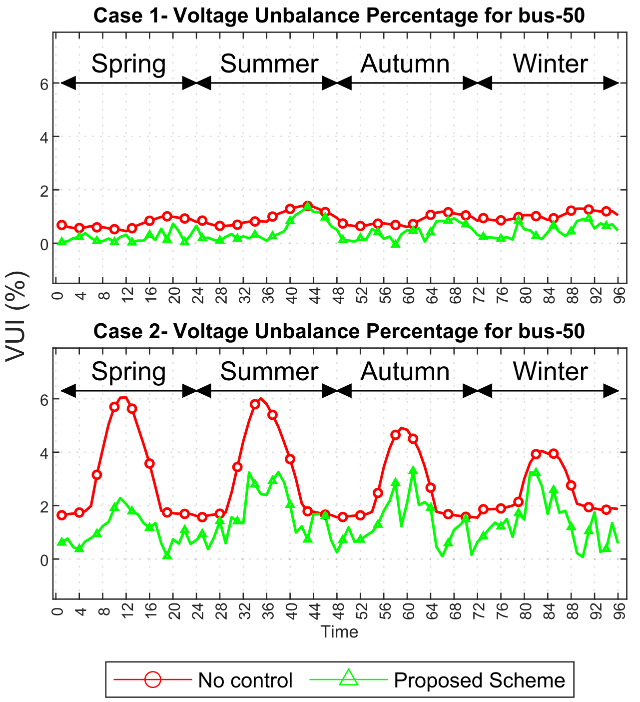

FIGURE 13. Evaluation of improvement in voltage unbalance in both test cases.

that the values of the voltage unbalance index, after the application of the proposed voltage control scheme, is less than five percent which is in accordance with ANSI standards.

All the results for both test cases prove the robustness and efficiency of the proposed real-time, coordinated decentralized voltage regulation scheme for unbalanced distribution networks with different numbers of renewable DGs on different phases. The results also demonstrate the reduction in the magnitude of voltage unbalance in the case of the highly unbalanced distribution system.

V. CONCLUSION

In this paper, a new adaptive clustering-based distributed voltage regulation scheme is presented for the unbalanced distribution systems. The scheme effectively regulated the voltage in a decentralized manner with minimal communication requirements by segregating the distribution feeder into smaller dynamic and adaptive control zones based on the number and controlling power of potentially active DGs. The proposed clustering algorithm ensured the inclusion of only high-sensitivity nodes for respective DGs rendering weak inter-zonal linkages. All the DGs were appointed as their own zone controllers, and no extra control infrastructure was required. A multi-objective optimization problem was designed for the reactive power optimization of DGs by power factor manipulation. The power factor optimization during the OLTC tap shift delay saved from excessive tap changes and possible hunting phenomena due to continuous variation in operational states of DGs. Later, by solving another optimization problem, taps were successfully selected for the OLTCs in two test cases on the IEEE 123-node test feeder. VQF and VUI values show significant improvements after the application of the proposed scheme. The system self-managed itself and optimally utilized the potential of DG units without compromising their generation capacity in the form of active power curtailment or power network stability due to excessive DG penetration. To sum up, the proposed coordinated real-time decentralized voltage control schemes can be effectively utilized to solve the stability issues arising from overvoltages due to increasing levels of distributed generation in unbalanced distribution networks.

REFERENCES

[1] A. Irena, "Renewable capacity highlights," in *Proc. Int. Renew. Energy Agency (IRENA)*, 2020, pp. 1–8.
[2] S.-E. Razavi, E. Rahimi, M. S. Javadi, A. E. Nezhad, M. Lotfi, M. Shafie-Khah, and J. P. S. Catalão, "Impact of distributed generation on protection and voltage regulation of distribution systems: A review," *Renew. Sustain. Energy Rev.*, vol. 105, pp. 157–167, May 2019.
[3] S. Yousuf and A. Vajuhudeen, "Current communication media in power system," *Int. J. Res. Electr. Eng.*, vol. 4, no. 2, pp. 145–147, 2017.
[4] *IEEE Standard for Interconnecting Distributed Resources With Electric Power Systems*, IEEE Standard 1547^{TM}, 2009.
[5] K. E. Antoniadou-Plytaria, I. N. Kouveliotis-Lysikatos, P. S. Georgilakis, and N. D. Hatziargyriou, "Distributed and decentralized voltage control of smart distribution networks: Models, methods, and future research," *IEEE Trans. Smart Grid*, vol. 8, no. 6, pp. 2999–3008, Nov. 2017.
[6] D. Stanelytė and V. Radziukynas, "Analysis of voltage and reactive power algorithms in low voltage networks," *Energies*, vol. 15, no. 5, p. 1843, Mar. 2022.
[7] S. Poudel, M. Mukherjee, and A. P. Reiman, "A fairness-based distributed energy coordination for voltage regulation in distribution systems," in *Proc. IEEE Green Technol. Conf. (GreenTech)*, Mar. 2022, pp. 45–50.
[8] K. K. Mehmood, S. U. Khan, S.-J. Lee, Z. M. Haider, M. K. Rafique, and C.-H. Kim, "A real-time optimal coordination scheme for the voltage regulation of a distribution network including an OLTC, capacitor banks, and multiple distributed energy resources," *Int. J. Electr. Power Energy Syst.*, vol. 94, pp. 1–14, Jan. 2018.
[9] T. Tewari, A. Mohapatra, and S. Anand, "Coordinated control of OLTC and energy storage for voltage regulation in distribution network with high PV penetration," *IEEE Trans. Sustain. Energy*, vol. 12, no. 1, pp. 262–272, Jan. 2021.
[10] K. W. Joung, T. Kim, and J.-W. Park, "Decoupled frequency and voltage control for stand-alone microgrid with high renewable penetration," *IEEE Trans. Ind. Appl.*, vol. 55, no. 1, pp. 122–133, Jan. 2019.
[11] Z. Tang, D. J. Hill, and T. Liu, "Distributed coordinated reactive power control for voltage regulation in distribution networks," *IEEE Trans. Smart Grid*, vol. 12, no. 1, pp. 312–323, Jan. 2021.
[12] J. Zhao, M. Yao, H. Yu, G. Song, H. Ji, and P. Li, "Decentralized voltage control strategy of soft open points in active distribution networks based on sensitivity analysis," *Electronics*, vol. 9, no. 2, p. 295, Feb. 2020.
[13] A. Andreotti, A. Petrillo, S. Santini, A. Vaccaro, and D. Villacci, "A decentralized architecture based on cooperative dynamic agents for online voltage regulation in smart grids," *Energies*, vol. 12, no. 7, p. 1386, Apr. 2019.
[14] J. Schiffer, T. Seel, J. Raisch, and T. Sezi, "Voltage stability and reactive power sharing in inverter-based microgrids with consensus-based distributed voltage control," *IEEE Trans. Control Syst. Technol.*, vol. 24, no. 1, pp. 96–109, Jan. 2016.
[15] D. Ranamuka, A. P. Agalgaonkar, and K. M. Muttaqi, "Online voltage control in distribution systems with multiple voltage regulating devices," *IEEE Trans. Sustain. Energy*, vol. 5, no. 2, pp. 617–628, Apr. 2014.
[16] A. M. Amani, N. Gaeini, M. Jalili, and X. Yu, "Voltage control in distributed generation systems based on complex network approach," *Energy Proc.*, vol. 110, pp. 334–339, Mar. 2017.
[17] A. Kulmala, S. Repo, and P. Järventausta, "Coordinated voltage control in distribution networks including several distributed energy resources," *IEEE Trans. Smart Grid*, vol. 5, no. 4, pp. 2010–2020, Jul. 2014.

[18] M. Dashtdar and M. Dashtdar, "Voltage control in distribution networks in presence of distributed generators based on local and coordinated control structures," *Sci. Bull. Electr. Eng. Fac.*, vol. 19, no. 2, pp. 21–27, Oct. 2019.
[19] D. Pappalardo, V. Calderaro, and V. Galdi, "Microgrids-based approach for voltage control in distribution systems by an efficient sensitivity analysis method," *IEEE Syst. J.*, vol. 16, no. 3, pp. 4210–4221, Sep. 2022.
[20] P. Li, H. Su, L. Yu, Z. Liu, C. Wang, and J. Wu, "Voltage control method of distribution networks using PMU based sensitivity estimation," *Energy Proc.*, vol. 158, pp. 2707–2712, Feb. 2019.
[21] H. Ji, H. Yu, G. Song, P. Li, C. Wang, and J. Wu, "A decentralized voltage control strategy of soft open points in active distribution networks," *Energy Proc.*, vol. 159, pp. 412–417, Feb. 2019.
[22] H. Xu, A. D. Domínguez-García, V. V. Veeravalli, and P. W. Sauer, "Data-driven voltage regulation in radial power distribution systems," *IEEE Trans. Power Syst.*, vol. 35, no. 3, pp. 2133–2143, May 2020.
[23] Y. Li, Y. Feng, H. Zhang, Y. Cao, and C. Rehtanz, "An adaptive zone-division approach for voltage control of power grid with distributed wind farms: A case study of a regional power grid in central south China," *Int. J. Electr. Power Energy Syst.*, vol. 103, pp. 652–659, Dec. 2018.
[24] R. Sepehrzad, M. Khojasteh Rahimi, A. Al-Durra, M. Allahbakhshi, and A. Moridi, "Optimal energy management of distributed generation in micro-grid to control the voltage and frequency based on PSO-adaptive virtual impedance method," *Electr. Power Syst. Res.*, vol. 208, Jul. 2022, Art. no. 107881.
[25] L. Wang, A. Dubey, A. H. Gebremedhin, A. K. Srivastava, and N. Schulz, "MPC-based decentralized voltage control in power distribution systems with EV and PV coordination," *IEEE Trans. Smart Grid*, vol. 13, no. 4, pp. 2908–2919, Jul. 2022.
[26] Z. Tang, D. J. Hill, and T. Liu, "Distributed control of active distribution networks to support voltage control in subtransmission networks," *Int. J. Electr. Power Energy Syst.*, vol. 117, May 2020, Art. no. 105715.
[27] V. Calderaro, G. Conio, V. Galdi, G. Massa, and A. Piccolo, "Optimal decentralized voltage control for distribution systems with inverter-based distributed generators," *IEEE Trans. Power Syst.*, vol. 29, no. 1, pp. 230–241, Jan. 2014.
[28] V. Alimisis and P. C. Taylor, "Zoning evaluation for improved coordinated automatic voltage control," *IEEE Trans. Power Syst.*, vol. 30, no. 5, pp. 2736–2746, Sep. 2015.
[29] P. Cuffe and L. F. Ochoa, "A voltage control scheme for generation-dominated networks to maximize power export," *IEEE Trans. Power Syst.*, vol. 33, no. 6, pp. 7321–7323, Nov. 2018.
[30] S. K. Sheikh Abdullah, "Adaptive zoning in coordinated voltage control system applications for TNB network system," *Int. J. Simul., Syst., Sci. Technol.*, vol. 10, pp. 1–51, Jan. 2016.
[31] D. Kiran, A. R. Abhyankar, and B. K. Panigrahi, "Hierarchical clustering based zone formation in power networks," in *Proc. Nat. Power Syst. Conf. (NPSC)*, Dec. 2016, pp. 1–6.
[32] C. Li, V. R. Disfani, Z. K. Pecenak, S. Mohajeryami, and J. Kleissl, "Optimal OLTC voltage control scheme to enable high solar penetrations," *Electr. Power Syst. Res.*, vol. 160, pp. 318–326, Jul. 2018.
[33] K. K. Mehmood, C.-H. Kim, S. U. Khan, and Z. M. Haider, "Unified planning of wind generators and switched capacitor banks: A multiagent clustering-based distributed approach," *IEEE Trans. Power Syst.*, vol. 33, no. 6, pp. 6978–6988, Nov. 2018.
[34] National Renewable Energy Laboratory. (2017). [Online]. Available: https://developer.nrel.gov/docs/solar/nsrdb/psm3-download/

RABBAYA AKHTAR received the B.S. degree from COMSATS University Islamabad, Wah Campus, Pakistan, in 2017, and the M.S. degree in electrical engineering from the National University of Sciences and Technology, Islamabad, Pakistan, in 2022.

From 2017 to May 2023, she was a Laboratory Engineer with Air University, Islamabad. Subsequently, since June 2023, she has been an Assistant Manager (technical) with National Transmission and Despatch Company. Her research interests include electrical power systems, machine learning, and electric vehicles.

REHAN NAWAZ received the B.S. and M.S. degrees in electrical engineering from Air University, Islamabad, Pakistan, in 2015 and 2017, respectively, where he is currently pursuing the Ph.D. degree.

From 2015 to 2021, he was a Research Assistant with Air University. Since 2021, he has been a professional freelancer on UPWORK. His research interests include electrical power systems, machine learning, deep learning, security, and reliability of cyber physical systems.

KHAWAJA KHALID MEHMOOD received the B.Sc. degree in electrical power engineering from the Mirpur University of Science and Technology, Mirpur, Pakistan, in 2012, and the Ph.D. degree in electrical power engineering from Sungkyunkwan University, South Korea, in 2019. He is currently a Postdoctoral Researcher with the Department of Electrical Engineering, Eindhoven University of Technology, Eindhoven, The Netherlands. He is also an Assistant Professor with The University of Azad Jammu and Kashmir, Muzaffarabad, and the U.S.–Pakistan Center for Advanced Studies in Energy (USPCAS-E), National University of Sciences and Technology, Islamabad, Pakistan. His research interests include planning and operations of active distribution systems, machine learning applications in distribution systems, electric vehicles, and battery energy storage systems.

SYED BASIT ALI BUKHARI received the B.Sc. degree from The University of Azad Jammu and Kashmir, Muzaffarabad, Pakistan, the master's degree in electrical power engineering from the University of Engineering and Technology, Taxila, Pakistan, and the Ph.D. degree in electrical power engineering from Sungkyunkwan University, South Korea. He is currently an Assistant Professor with the Department of Electrical Engineering, The University of Azad Jammu and Kashmir. He was an Assistant Professor with the U.S.–Pakistan Center for Advanced Studies in Energy (USPCAS-E), National University of Sciences and Technology, Islamabad, Pakistan. His research interests include protection and islanding detection of active distribution systems, machine learning applications in distribution systems, microgrid, and smart grids.

ABDUL WADOOD received the B.S. degree in electronic engineering from the University of Engineering and Technology, Peshawar, Pakistan, in 2012, the master's degree in electrical engineering from the Sarhad University of Science and Information Technology, Peshawar, in 2015, and the Ph.D. degree from the Department of Electrical Engineering, Yeungnam University, Gyeongbuk, South Korea, in 2019. He is currently an Assistant Professor with the Department of Electrical Engineering, Air University, Islamabad, Pakistan. His areas of interests include power system relaying, power system protection, energy management systems, renewable energy, evolutionary, and metaheuristic algorithms.

KASHIF IMRAN received the B.Sc. and M.Sc. degrees in electrical engineering from the University of Engineering and Technology (UET), Lahore, in 2006 and 2008, respectively, and the Ph.D. degree in electrical engineering from the University of Strathclyde, in 2015.

He was with the Transmission and Distribution Division, SIEMENS, and the Power Distribution Design Section, NESPAK, from 2006 to 2007. He was a Faculty Member with UET and COMSATS University, Lahore. He was the Inaugural Head of the Department of Electrical Power Engineering, U.S.–Pakistan Center for Advanced Studies in Energy (USPCASC-E), National University of Sciences and Technology (NUST), Islamabad, from 2018 to 2021, where he is currently an Associate Professor. He received the Commonwealth Scholarship for his Ph.D. research. His primary research interests include energy policy, optimization for power systems, electricity markets operations and planning, and power system protection.

TAHIR KHURSHAID received the B.E. degree in electrical engineering from Jammu University, India, in 2011, the master's degree in power system engineering from Galgotias University, Greater Noida, India, in 2014, and the Ph.D. degree in electrical engineering from the Department of Electrical Engineering, Yeungnam University, South Korea. He is currently an Assistant Professor with the Department of Electrical Engineering, Yeungnam University. His research interests include power system protection, power system optimization, power system analysis and design, and power system deregulation.

KI-CHAI KIM (Member, IEEE) received the B.S. degree in electronic engineering from Yeungnam University, Gyeongsan, South Korea, in 1984, and the M.S. and Doctor of Engineering degrees in electrical engineering from Keio University, Japan, in 1986 and 1989, respectively. He was a Senior Researcher with the Korea Standards Research Institute, South Korea, in 1993, working in electromagnetic compatibility. From 1993 to 1995, he was an Associate Professor with the Fukuoka Institute of Technology, Fukuoka, Japan. Since 1995, he has been with Yeungnam University, where he is currently a Professor with the Department of Electrical Engineering. He was the President of the Korea Institute of Electromagnetic Engineering and Science (KIEES), in 2012. His research interests include EMC/EMI antenna evaluation, electromagnetic penetration problems in slots, and applications of electromagnetic field and waves. He received the 1988 Young Engineer Awards from the Institute of Electronics, Information and Communication Engineers (IEICE), Japan; and the Paper Presentation Awards from the Institute of Electrical Engineers (IEE), Japan, in 1994.